The influence of oxygen containing functional groups on carbon fibers for mechanical properties and recyclability of CFRTPs made with in-situ polymerizable polyamide 6

Toshihira Irisawa [a), *], Ryohei Inagaki [a)], Junya Iida [a)], Ryosuke Iwamura [a)],Kento Ujihara [a)], Sarasa Kobayashi [a)] and Yasuhiro Tanabe [a)]

[a)] Graduate School of Engineering, Nagoya University, Furo-cho, Chikusa-ku, Nagoya 464-8603, Japan.

[*]Corresponding author, E-mail: Toshihira Irisawa, irisawa.toshihira@material.nagoya-u.ac.jp

Abstract

The influence of the oxygen containing functional groups on carbon fibers for mechanical properties and recyclability of carbon fiber reinforced thermos-plastics (CFRTPs) made with in-situ polymelizable polyamide 6 (PA6) have been discussed. Interfacial adhesion between CFs with functional groups and PA6 became higher compared with that of because of the interaction such as hydrogen bond, covalent bond. Furthermore, it was revealed that these effects apparently improved the mechanical properties of the CFRTPs. On the other hand, the interaction between the functional groups and PA6 affected the recyclability of the CFRTPs. Although PA6 as the matrix polymer of the CFRTP could be pyrolyzed even under N_2 gas and recycle CFs with very little char could be obtained at 600 ^oC, it was found that the tensile strength decreased after pyrolytic process by about 10 % only when the CFs with the functional groups were used for reinforcement fibers.

Keyword: A; Carbon Fibers, Thermoplastic resin, B; Interface/interphase, E; Recycling

1. Introduction

Carbon fiber reinforced plastics (CFRPs) have already been used for various applications [1,2], and the demand for the CFRPs as latest automotive application is considered in terms of weight saving of the structural materials for body. It is important for energy saving and carbon reduction to shift to CFRPs as the materials [3,4]. Low viscosity monomers which show good impregnation into the carbon fibers (CFs) are used to produce commercially available high quality carbon fiber reinforced thermosetting resins (CFRTSs). However, the CFRTSs are very expensive materials because the molding time is extremely long and the productive energy is high due to the heat setting of thermoset resins [4]. On the other hand, Carbon fiber reinforced thermoplastics (CFRTPs) have been focused on their low cost and high production rate because they can be produced speedily by using hot-melt methods. Therefore, many investigations about CFRTPs have been performed from various directions [3-20]. Especially, commodity thermoplastics such as polypropylene (PP) or low cost engineering thermoplastics such as polyamide (PA) or polycarbonate are selectively used as the matrix resin for CFRTPs in automotive applications. However, the CFRTPs have various drawbacks such as the impregnability of thermoplastics into CFs fabrics or the interfacial adhesion between CFs and thermoplastics [4-8,10-20].

The surface of commercial CFs has oxygen containing functional groups by an electrolytic oxidation treatment. The purpose of this treatment is improving the interfacial adhesion between CFs and epoxy resin by forming covalent bonds [9,21]. On the other hand, thermoplastics cannot form the covalent bonds with CFs during the hot-melt methods, so the improvement of interfacial adhesion for CFRTPs is a critical issue [4,10-12]. However, it is difficult to modify the fabrication procedure of CFs including the surface treatment process, so it is desired to develop novel techniques to improve the interfacial adhesion among oxygen containing functional groups and thermoplastics. Therefore, the investigation about the effects of the functional groups for some thermoplastics has been done [4,10-12], and it was indicated that interfacial adhesion between PA6 and CFs having the oxygen containing functional groups by the hot-melt method became relatively high, because PA6 is a polar polymer [6,12]. However, the effect of the functional groups has not been studied quantitatively.

As for the impregnability of CFRTPs, the impregnation of thermoplastics into CFs fabrics is difficult because the melt viscosity of thermoplastics is higher than that of thermoset resin in the condition of monomer [4, 16-20]. One possible solution to this problem is the molding of discontinuous CFRTPs applied kneading process. It was reported that the discontinuous CFRTPs were molded in minutes by the hot-press or injection molding [13-15], while the reinforcement effect of discontinuous fibers is extremely low. Therefore, the development of continuous CFRTPs in terms of impregnation has also been performed; e.g., the powder-impregnation method [16], the methods to use CFs tow widely opened [17], and the method to use CFs/thermoplastic fibers commingled yarns [18]. As an entirely different method, molding CFRTPs made with in-situ polymerizable PA6 by a vacuum assisted resin transfer molding (Va-RTM) has been proposed [19,20]. In this method, ε-caprolactam with low viscosity can be impregnated into CFs fabrics and polymerized to PA6. Therefore, CFRTPs made with in-situ polymerizable PA6 shows good impregnation. Furthermore, they also reported that this process preserved high productivity as the merit of CFRTPs for the polymerization reaction time is a few minutes. On the other hand, it is thought the interface formed by using in-situ polymerizable PA6 in CFRTPs is different from that formed by using melting PA6 for different solidification mechanism. However, there is no reports about the investigation of interfacial adhesion between CFs and in-situ polymerizable PA6.

In this study, to verify the potential of CFRTP made with in-situ polymerizable PA6 we focused on three topics about it: interfacial adhesion, difference of molding method, and recycling. To discuss the interfacial adhesion, the interfacial adhesion and mechanical properties of CFRTPs which made of different surface treatment CFs was explored. To confirm the difference of molding method, interfacial adhesion between in-situ polymerization and hot-melt method was compared. It is anticipated that the loss and waste of CFRPs will increase with the demand expansion of CFRPs, and the development of recycle technologies for CFRPs is urgently required [22-24]. To considering potential of recycling of CFRTPs made with in-situ polymerizable PA6, recover CFs (recycle CFs; Re-CFs) were derived from the CFRTPs using pyrolytic process which is one of methods to separate, and their mechanical properties and the surface condition were observed.

2. Experimental

2.1. Materials

In-situ polymerizable PA6 containing the catalyst and active agent supplied by Nagase ChemteX Corporation was used as a matrix polymer. Plain fabrics of PAN-based CFs (T700-12K, Toray Industries, Inc.) were used as the reinforcement fibers. Prepared CFs have oxygen containing functional groups by a surface treatment and sizing agent on the surface details of which are not known. It is reported that the sizing agent interferes with the impregnation of the PA6 at the state of monomer [19-20]. Total flow chart of preparation of CFs and CFRTPs are shown in Fig. 1. Firstly, the CFs fabrics were washed in acetone for 45 min and immediately washed again for 5min in replaced acetone to remove the sizing agent. CFs surface was observed by using field emission scanning electron microscope (SEM) (E-1010, Hitachi), and it was confirmed that the sizing agent was almost removed. These CFs code Fre-with-CFs. To compare the effects of the functional groups, CFs without the functional groups and CFs with the oxygen containing functional groups again by the publicized surface treatment were prepared as follows; Fre-CFs fabrics were heat-treated at 1000 ^{o}C in Ar gas for 3h for decomposition of the oxygen containing functional groups (Fre-without-CFs). And then, Fre-without-CFs fabrics which size is 80 x 160 mm were surface-treated by using the ultraviolet light (Sun Energy CORP.) and ozone (UV-O_3) treatment. The distance from CFs fabrics to UV light was set at 150 mm in chamber filled with O_3 gas. The power of UV light was 120 W. Both sides of the CFs fabrics were irradiated for 15 min, respectively. Finally, the CFs fabrics with oxygen containing functional group were obtained again (Fre-with-UV-CFs).

2.2. Molding method of CFRTPs

CFRTPs consisted with in-situ polymerizable PA6 and each Fre-CFs (Fre-without-CFs/CFRTP, Fre-with-CFs/CFRTP and Fre-with-UV-CFs/CFRTP) were molded by Va-RTM method as follows (Fig. 2); Three fabrics sheets cutted into 80 x 160 mm were cross-ply stacked in a mold set into a vacuum-sealed package. PA6 before the polymerization (ε-caprolactam) were dried at 45 ^{o}C for 1 day in a vacuum oven for the removing the absorbed water and immediately melted at 110 ^{o}C.

The ε-caprolactam were impregnated into CFs fabrics with assistance of vacuum and the mold was transferred to the hot-press machine. It was already reported that the optimized condition for polymerization of this CFRTPs was at 140 - 160 °C [19]. Therefore, the hot-press machine was set at 160 °C and pressed under 0.15 MPa for 5 min. The mold was naturally cooled and then each CFRTPs with the thickness of about 1.5 mm. The volume fraction of fiber was measured following JIS K7075.

2.3. Mechanical properties of CFRTPs

The mechanical properties of CFRTPs were evaluated by tensile and 3-point bending test (AG-X plus, Shimadzu corp.). The specimen size of 160 mm x 7 mm x 1.5 mm was for the tensile test and that of 85 mm x 10 mm x 1.5 mm for the bending test; the longitudinal direction was along 0° in the stacking. For the tensile test, specimen ends were sandwiched with aluminum tabs and the end-tabs were gripped. The test was carried out at a strain gage length of 50 mm and a tensile rate of 1 mm/min at room temperature. The bending test was carried out with 65 mm distance of lower supports at a rate of 5 mm/min under room temperature. The diameter of indenter was 5mm. Each modulus (E_c) and strength (σ_c) were determined from the initial slope of a stress-strain (S-S) curve in the strain range from 0.1 to 0.6 % and the maximum stress at the specimen break from tensile and bending tests, respectively.

2.4. Crystallinity of matrix polymer in CFRTPs

The crystallinity of matrix polymer in CFRTPs was evaluated by differential scanning calorimetry (DSC) (Q-2000, TA Instruments). DSC measurement was carried out from room temperature to 280 °C at a heating rate and cooling rate of 10 °C min^{-1}. The melting temperature (T_m) and the crystallization temperature (T_c) of PA6 were determined as the peak temperatures of DSC curves measured during the first heating and the first cooling processes, respectively. The degree of crystallinity of PA6 (X_c) was calculated according to the equation (1) where ΔH_m is the specific melting heat calculated from the endothermic peak area in the heating process, $\Delta H_{m,o}$ is the specific melting heat of PA6 crystal, and m is the mass fraction of CFs [25].

$$X_C = \frac{\Delta H_m}{\Delta H_{m,0}(1-m)} \times 100 \qquad (1)$$

The values of $\Delta H_{m,o}$ for the α and γ phases are 241 Jg^{-1} and 239 Jg^{-1} respectively, and the average value (240 Jg^{-1}) was used for $\Delta H_{m,o}$ in this study [25-27].

2.5. Molecular weight of matrix polymer in CFRTPs

Molecular weight of matrix polymer in CFRTPs was evaluated by gel permeation chromatography (GPC) (HLC-8320GPC, Tosoh corp.) (ISO 16014-1). PA6 in CFRTP was dissolved into 2,2,2-Trifluoroethanol and was measured at the flow rate of 1.0 mL/min under room temperature. The molecular weight was calculated as a weight-average molecular weight (M_w).

2.6. Interfacial adhesion in CFRTPs

The interfacial adhesion between CF and PA6 can be quantified as interfacial shear strength (IFSS) by the fragmentation methods [9,28-30]. The fragmentation test under a microscope was carried out using a tensile testing machine at room temperature. The specimen was prepared as follows (Fig. 3(a)); A single CF embedded PA6 films was prepared by Va-RTM at 160 ºC for 5 min (CF/PA6-RTM). Then, the film was cut into the strip specimen geometry with 30 mm x 2.5 mm. The specimen was tested at a gage length of 15 mm and a rate of 1 mm/min until the fragmentation process was saturated, which was about 10 % of the tensile strain. The average length of fragmented CFs ($<L>$) was obtained over 70 measurements in each sample and the test was carried out for 5 specimens. IFSS was calculated by the following equation.

$$\text{IFSS} = \frac{D\sigma_{f,l_c}}{2l_c} \qquad (2)$$

The ineffective length (l_c) can be obtained as follows:

$$< L >= \frac{3}{4} l_c \qquad (3)$$

The measurement methods of an average diameter (D) and the tensile test methods for estimation of strength ($\sigma_{f,lc}$) are explained in 2.6. $\sigma_{f,lc}$ was needed to be estimated as the tensile strength of CFs at the length of l_c. Therefore, the tensile tests were carried out for 50 specimens and the Weibull analysis of tensile strength obtained from the single fiber tensile test were performed, and $\sigma_{f,lc}$ was estimated [9,29,30]. The IFSS of CF/Epoxy prepared by Va-RTM (CF/Epo-RTM), CF/PP and CF/PA6 prepared by

melting methods (CF/PP-melt, CF/PA6-melt) (Fig. 3(b)) was also measured for comparison as thermoset and other thermoplastic matrix resins. The bisphenol-A type resin (jER-828, Mitsubishi Chemical corp.) was used as a base resin and boron trifluoride monoethyl amine (Stella Chemifa Corp.) was used as a hardener of epoxy resin. PP (J-107 G, Prime Polymer Co., Ltd.) and PA6 (CM1001, Toray Industries, Inc.) films for melting methods were prepared in advance, respectively.

2.7. Pyrolytic process to recover CFs from CFRTP

Fre-with-CFs/CFRTP, Fre-without-CFs/CFRTP and Fre-with-UV-CFs/CFRTP molded by Va-RTM method were pyrolyzed for decomposition of matrix in a tubular furnace, respectively (Fig. 4). Firstly, CFRTPs were put at one side of furnace to prevent unnecessary heat treatment. And then, they were pushed into the soaking area by using Inconel stick, and were heat-treated at the optimized condition (in N_2 gas under 600 ^oC for 30 min). The detail of optimized condition for the pyrolytic process optimized by the thermal gravimetric analysis (TGA) (Q-500, TA Instruments) and the field-emission scanning electron microscope (FE-SEM) (JSM-7500FA, JEOL, Ltd.) will be discussed in the section of results and discussion. TGA measurements were carried out from 200 to 700 ^oC at a heating rate of 20 $^oC\ min^{-1}$ under N_2 gas. Three Re-CFs (Re-without-CFs, Re-with-CFs and Re-with-UV-CFs) were finally obtained, respectively.

2.8. Properties of CFs

Single fiber tensile tests were performed for the comparison of mechanical properties of each CF. The tensile tests were carried out for 50 specimens under ISO-11566. The test was operated at a gage length of 25 mm and a crosshead speed of 1 mm/min. The fiber diameter was measured by using the diffraction of a He-Ne laser beam normal incident on the fiber under ISO-11567. The tensile strength (σ_f) was determined as the maximum stress of S-S curve. In order to accurately determine the tensile modulus (E_f), compliance correction was performed according to ISO-11566. For the evaluation of crystallite size and structural parameters of each CFs, the density (d) was measured by the sink-float method (ISO-10119) and Wide-angle X-ray diffraction (WAXD) by using nickel-filtered CuKα radiation was

carried out [31]. The X-ray beam was incident perpendicular to the fiber axis of aligned fibers. The average interlayer spacing (d_{002}) and carbon layer stack height (L_c) were estimated from (0 0 2) diffraction profile using Bragg and Scherrer equations. From the full-width at half-maximum intensity (FWHM) of the azimuthal angle scan of (0 0 2) diffraction, the crystal orientation parameter (f), which is defined as (1-FWHM)/π, was also estimated [31]. Surface conditions of CFs were evaluated as the O/C value (the peak area ratio of O_{1s} and C_{1s}) by using X-ray Photoelectron Spectroscopy (XPS) (PHI5000 Versa ProbeII, Ulvac-Phi, Inc.) and were observed by using SEM. IFSS of CF/PA6-melt by using each Re-CFs was also measured by the fragmentation method.

3. Results and discussion

3.1. The dependence on the molding methods for interfacial adhesion

Before the discussion of the effects of oxygen containing functional groups for CFRTPs, each Fre-CF used as the reinforcement fibers is summarized. The tensile properties, density, crystallite parameter from WAXD and O/C value from XPS are shown in Table 1. The O/C value is the index of volume of oxygen containing functional groups. Therefore, it is found that functional groups could be pyrolytically removed from Fre-without-CFs. Subsequently, it was reported that UV-O_3 treatment efficiently works as the method of surface oxidation for CFs [32], Fre-with-UV-CFs also partly regained the functional groups in our method of UV-O_3 treatment although the O/C value was lower than that of Fre-with-CFs. To discuss the pure effects of the functional groups on the interfacial adhesion, it is desired that the CFs keep their mechanical properties regardless of their treatments. It is clear that the tensile modulus of each Fre-CF could be obtained with constant values in Table 1. It is known that the tensile modulus of CFs generally relates to the crystallinity, crystal orientation and voids volume [33,34]. The interlayer spacing and layer stack height reflect the crystallinity of CFs, and density is related to the crystallinity and voids volume. Each parameter did not change regardless of each treatment, so it was confirmed that the tensile modulus of each Fre-CFs was the same in view point of CFs structure. In contrast, the tensile strength decreased slightly after heat-treatment, although the treatment was performed

under Ar gas. It might be due to the introduction of defects during the heat-treatment. On the other hand, the tensile strength of Fre-with-UV-CFs showed the same value with that of Fre-without- CF.

The IFSSs of CF/PA6-RTM and CF/PA6-melt by using each Fre-CF were shown in Fig. 5. For the comparison, the IFSSs of CF/Epo-RTM and CF/PP-melt by using Fre-with-UV-CFs were also shown. The IFSS for CF/Epo-RTM was the highest, followed in order by those for PA6 and PP. As the comparison among Fre-CFs for CF/PA6, the IFSS for Fre-CFs with the oxygen containing functional groups were higher than that of Fre-without-CFs. Furthermore, as the comparison to CF/PA6-RTM and CF/PA6-melt, the IFSS for in-situ polymerizable by using RTM showed higher than that of hot-melt in all Fre-CFs.

In the case of CF/Epo-RTM, it is thought that epoxy resin made the covalent bonds with the oxygen containing functional groups on the CFs during the curing induced by chemical reaction. Therefore, CF/Epo-RTM had the highest IFSS. However, the thermoplastics can hardly be expected to make the covalent bonds with them during the physical state variation. In addition, the interaction between PP and the functional groups on the CFs are weak because there are no polar parts in PP. Therefore, it is thought that CF/PP-melt had the lowest value in spite of using the Fre-with-CFs. On the other hand, it is expected that some kind of interaction between CF/PA6 efficiently works for the interfacial adhesion. In the case of CF/PA6-melt, the hydrogen bonds might be formed between the functional groups on the CFs and the amide bonds into polymer chain structure of PA6. Therefore, it is considered that IFSS of CF/PA6-melt was quite higher than that of CF/PP-melt. Moreover, it is clear that the functional groups on the CFs efficiently work for the interfacial adhesion of CF/PA6-melt, comparing the IFSS of CFs with and without the functional groups. In the case of CF/PA6-RTM, not only hydrogen bonds but also two other factors are also considered for the reason of higher IFSSs. The first factor is forming of the covalent bonds between CFs and in-situ polymerizable PA6, because polymerization was occurred during the molding by CF/PA6-RTM. The second factor is the difference of residual stress between hot-melt method and RTM methods. While the effect of residual stress may have time dependence for stress relaxation, we cannot confirm this effect in this study. Although the contribution ratio of each effect to interfacial adhesion is uncertain at the present stage, IFSS of CF/PA6-RTM became

higher than that of CF/PA6-melt for these effects. Furthermore, it is also found that the interfacial adhesion is saturated at a certain amount of functional groups.

3.2. The effects of interfacial adhesion for the CFRTPs

The melting temperature, crystallization temperature, crystallinity and the weight-average molecular weight of PA6 into each CFRTP were summarized in Table 2. For the comparison, the values of in-situ polymerizable PA6 itself (Neat-PA6-RTM) were also shown. The melting temperatures of all CFRTP and Neat-PA6-RTM were almost the same, so the CFs themselves or the oxygen containing functional groups on the surface of CFs did not influence the melting behavior. On the other hand, from results of molecular weight of CFRTPs, PA6 had high molecular weight by containing CFs. Moreover, using CFs with the functional groups, molecular weight of PA6 showed higher value than that of CFs without the functional groups. It was reported that the ring-opening polymerization of ε-caprolactam, which is the same grade as in-situ polymerizable PA6 in this study, is initiated from isocyanate compounds [19,20]. In this case, the functional groups on surface of CFs might work as initiator like isocyanate compounds, so the covalent bonds might be formed between in-situ polymerizable PA6 and CFs. It is thought that these facts also support the reason why the IFSS of CF/PA6-RTM was higher than that of CF/PA6-melt as mentioned above. Furthermore, PA6 had lower crystallization temperature and crystallinity by containing CFs. In the case of CFs with functional groups, the crystallization temperature and crystallinity decreased from the case of without the functional groups. It is thought that the high interfacial adhesion means the attachment of the polymer chain to the CFs surface, and prevents the rearrangement of polymer chain for crystallization. Therefore, the crystallization temperature and crystallinity decreased in the case of presence of CFs with the functional groups.

The average tensile/bending modulus, strength and volume fraction of fiber (V_f) of each CFRTP were listed in Table 3. The volume fractions of fiber of each CFRTP were almost same values, so the influence of the difference of them can be neglect. Both strength of CFRTPs using CFs with the functional groups (Fre-with-CFs/CFRTP, Fre-with-UV-CFs/CFRTP) showed higher value. The typical stress-strain (S-S) curves of tensile and bending test for each CFRTP were shown in Fig. 6 (a), (b).

During tensile test for Fre-without-CFs/CFRTP, high-pitched sound was continuously heard above the tensile stress of 300 MPa. Similarly, the S-S curve showed zigzag line above 300 MPa. It is considered to be the interfacial debonding because CF/PA6 into Fre-without-CFs/CFRTP has low IFSS. All CFRTPs were made of plain fabrics and fibers were not straight but woven. It is considered that the fracture occurred not in straight fibers parts by tensile deformation but around tilt fibers from loading axis by the shear deformation. The reason of many high pitch sounds was due to having many tilt fiber parts in CFRTPs. Therefore, the mechanical properties of CFRTPs were improved by enhancing IFSS, and the interfacial debonding results in low tensile strength of Fre-without-CFs/CFRTP.

The tensile modulus were almost constant regardless of the functional groups on CFs. On the other hand, the tensile modulus was evaluated from the initial slope of S-S curve which means that it is below 300 MPa, so it is thought that they were not affected by the interfacial debonding and all CFRTPs have almost constant values.

In the case of bending test, the remarkable difference of bending strength was observed. The fracture of Fre-without-CFs/CFRTP was occurred at about 300 MPa, and this stress is corresponding to the interfacial debonding stress of tensile test. Therefore, it is revealed that the bending fracture was strongly influenced by the interfacial debonding. Bending deformation consists of tensile and compression deformations. In the case of tensile deformation, shear fracture of tilt fibers parts does not affects the tensile strength of CFRTPs, however, in the case of compression deformation, that reduce compression strength of CFRTP, because the debonding makes fiber lateral support lost. For this reason, the bending strength was markedly decreased. Bending modulus of each CFRTP also had almost constant values for the same reasons as tensile test.

The mechanical properties of CFRTP may depend on the other factors: molecular weight, crystal structure and strength of CFs. However, it is thought that the influence of these factors was not so much in this study as the following reasons. Based on a rule of mixture, the effect of the mechanical properties of matrix resin is very small compared with that of reinforcement fiber, and the influence of mechanical properties of matrix polymer can be neglected. As shown in Table 1, although the tensile strength of Fre-with-UV-CFs decreased compared to the Fre-with-CFs because of the heat treatment, the

mechanical properties of Fre-with-CFs/CFRTP was the same as that of Fre-with-UV-CFs/CFRTP and the influence of CFs strength was limited to CFRTPs.

3.3. The effects of interfacial adhesion for recyclability of CFRTPs

To optimize the pyrolysis condition for CFRTP made with in-situ polymerizable PA6, the measurements of TGA under N_2 gas for Fre-with-CFs and Neat-PA6-RTM were performed. The TG curve of Fre-with-CFs were shown in Fig. 7(a). Although the slight weight loss of CFs was observed from 300 to 400 °C for the pyrolysis of sizing agent, the decomposition of CFs itself was not observed. Therefore, it is thought that the damage of Re-CFs could be prevented as much as possible. On the other hand, the TG curve of Neat-PA6-RTM were also shown in Fig. 7(b). The weight loss of Neat-PA6-RTM started from about 300 °C, and Neat-PA6-RTM could be pyrolyzed more than 99 % of its initial weight around 400 °C. The SEM images of Re-with-CFs pyrolyzed from Fre-with-CFs/CFRTP at temperature of 500, 550 and 600 °C for 30 min under N_2 gas were shown in Fig. 8 (a)- (c). Although Neat-PA6-RTM could be pyrolyzed more than 99 % of its initial weight around 400 °C, the remained char obviously existed at pyrolysis temperature of 550 °C. The actual tow of Re-with-CFs lost its flexibility due to agglutination between CFs. This condition inhibits the impregnation of matrix resins when Re-CFs reuse as reinforcement fiber for CFRTS or CFRTP. On the other hand, in the case of Re-with-CFs pyrolyzed at 600 °C, remained char was scarcely observed and Re-with-CFs had good flexibility. It was expected that the pyrolysis at 600 °C under N_2 gas prevents the damage for Re-CFs, so it was found that the optimized pyrolysis condition for CFRTPs made with in-situ polymerizable PA6 was set at the temperature of 600 °C under N_2 gas for 30 min. As the comparison, in the case of CFRTSs made with epoxy resin, it was reported that beginning decomposition temperature was above 400 °C, and epoxy resin could not be pyrolyzed completely and several % of char remained under N_2 gas [35]. Therefore, it is difficult to pyrolyze the CFRTSs under N_2 gas, so the investigations for the pyrolytic process for CFRTSs have been generally performed under air or superheated steam [24,35,36]. However, oxidation condition has the possibility of producing the damage to Re-CFs. Therefore, it is said that in-situ polymerizable PA6 can be

pyrolyzed easily from CFRTP without the severe damages under N_2 gas, so it is found that this CFRTPs PA6 has the advantage of recyclability by pyrolytic process compared with conventional CFRTSs.

As the summary of each Re-CFs, the tensile properties, density, crystallite parameter from WAXD and O/C value from XPS were shown in Table 4. Especially, comparisons of the tensile strength and O/C value of Re-CFs and Fre-CFs were also shown in Fig. 9, 10 as histogram. The tensile modulus of Re-CFs did not decrease after the pyrolytic process regardless of the functional groups on CFs. As mentioned above, the tensile modulus of CFs relates to the crystallinity, crystal orientation and voids volume. The interlayer spacing and layer stack height and density did not change compared with Table 1 and 4. In particular, it was known that the crystallite parameters of CFs were influenced with the maximum temperature in carbonization process [33]. Although the carbonization temperature generally sets up to 1000 - 1500 ^{o}C in the case of PAN-based CFs [23], the pyrolysis temperature in this study was decided at 600 ^{o}C. Therefore, it is thought that the pyrolytic process did not affect the crystallite parameter and the tensile modulus did not change after the process.

On the other hand, the pyrolytic process influenced the tensile strength of Re-CFs. Although the tensile strength of Fre-without-CFs and Re-without-CFs have almost constant values, the tensile strength of Re-with-CFs and Re-with-UV-CFs decreased compared with each Fre-CFs, respectively. It means that the tensile strength decreased after pyrolytic process only when the CFs with the oxygen containing functional groups on the surface were used as reinforcement fibers. It is difficult to decide the reasons of decreasing of the tensile strength during the pyrolytic process at the present stage. Actually, the obvious defects couldn't also be observed by using SEM. However, it was clear that the interaction between the functional groups and PA6 affected the decreasing of tensile strength because the small damages, even if being too small to be observed by SEM, were initiated on the surface during the pyrolytic process. Furthermore, it was found that the functional groups on the surface of Fre-with-CFs and Fre-with-UV-CFs decomposed after the pyrolytic process in terms of the O/C value.

Finally, to discuss the feasibility of reusing CFs as reinforcement fiber of CFRTP, the comparisons of IFSS of CF/PA6-melt by using each Fre-CF and Re-CF were shown in Fig. 11. The O/C values of Re-with-CFs, Re-with-UV-CFs and Re-without-CFs were below 0.07. In spite of smaller O/C

values, the IFSS of CF/PA6-melt by using Re-CFs were considerably high compared with the case by using Fre-CFs. The two possibilities are considered for the reason of higher IFSS of CF/PA6-melt by using Re-CFs. The one possibility is that the defects created during the pyrolytic process worked as the anchor effects. However, it is thought that this possibility was low because the IFSS were also high by using the Re-without-CFs and also the decreasing of strength wasn't observed after the pyrolytic process. The other possibility is that a little char on the surface after the pyrolytic process affected the IFSS as the anchor effects. Actually, a little char was also clearly observed on Re-CFs shown in Fig. 8(c). Furthermore, the roughness caused by other char which cannot be observed by using SEM may affect the IFSS. Therefore, it is concluded that the IFSS of CF/PA6-melt by using all Re-CFs were higher than that by using Fre-CFs. It is expected that these results become big merits for the reusing of Re-CFs for reinforcement fibers for CFRTP.

4. Conclusion

In this study, we explored interfacial adhesion, effects of molding method, and recycling of CFRTP made with in-situ polymerizable PA6.

The effects of oxygen containing functional groups to mechanical properties of CFRTP were investigated by preparing CFs with different carbon surface conditions. In the case of using the Fre-CFs, interfacial adhesion of CF/PA6 showed high interfacial shear strength for high interaction between CFs and PA6. The higher interfacial shear strength is due to forming the hydrogen bonds considering the interfacial shear strength using CFs without oxygen containing functional groups.

Effects of molding methods were evaluated by comparing interfacial shear strength and mechanical properties for CFRTPs using Va-RTM and melting method. The hydrogen bonds, the effect of residual stress, and the covalent bonds by polymerization during the molding were considered as controlling factors of interfacial shear strength and mechanical properties of CFRTPs. The latter two effects did not occur in conventional melting method, and it found that latter two effects are advantage of

the CFRTP made with in-situ polymerizable PA6. The mechanical properties of these CFRTPs were greatly improved and supported this assumption.

Using Pyrolytic process, recyclability of these CFRTPs was discussed. Different from the pyrolytic process of CFRTS which were performed under air or superheated steam, the matrix polymer in CFRTPs made with in-situ polymerizable PA6 was able to pyrolyze under N_2 gas. The tensile properties of Re-CFs were examined, and it is found that the tensile strength decreased after pyrolytic process in case of using CFs with the oxygen containing functional groups for reinforcement fibers. It is considered that the strong interaction between the functional groups and PA6 affected the carbon fiber surface for introducing the small damages during pyrolytic process.

As the summary, it is concluded that the CFRTPs made with in-situ polymerizable PA6 shows strong interaction between the surface of CFs and PA6, and good recyclability. These CFRTPs may be one of the candidate of structural materials replacing CFRTS and more research is needed.

Acknowledgements

This paper was supported by a future pioneering program commissioned by the New Energy and Industrial Technology Development Organization(NEDO). The authors are deeply indebted to the national composite center (NCC) of Japan. The materials used in this work are supplied by Nagase ChemteX Corporation.

References

1) Soutis C, Carbon fiber reinforced plastics in aircraft construction. Mater Sci Eng A 2005; 412(1-2): 171-176.
2) Grant A, Sporting composites. Reinf Plast 2005; 49(5): 46-49.
3) Takahashi J, III: Life cycle assessment and energy saving effect of CFRP. J Mater Sci Jpn 2008; 57(8): 852-855.
4) Zushi H, Tamura M, Ohsawa I, Uzawa K, Takahashi J, Yasuda H. Evaluation on mechanical properties of carbon fiber reinforced polypropylene. J Jpn Comp Mater 2006; 32(4): 153-162.
5) Offringa AR. Thermoplastic composites-rapid processing applications. Composites Part A 1996; **27**(4): 329-336.
6) Yan X, Imai Y, Nagata K, Sto K, Hotta Y. Relationship study between crystal structure and thermal/mechanical properties of polyamide 6 reinforced and unreinforced by carbon fiber from macro and local view. Polymer 2014; 55(23): 6186-2194.
7) Renzai F, Yunus R, Ibrahim NA, Mahdi ES. Development of short-carbon-fiber-reinforced polypropylene composite for car bonnet. Polym Plasi Technol Eng 2008; 47(4): 351-357.
8) Tanaka K, Kashihara H, Katayama T. Vacuum assisted high speed compression molding and evaluation of mechanical properties of continuous carbon fiber reinforced polycarbonate composite. J Soc Mater Sci Jpn 2011; 60(3): 251-258.
9) Irisawa T, Hashimoto R, Arai M, Tanabe Y. The suitability evaluation of aromatic amorphous thermoplastics as matrix resin for CFRTP having high thermal stability. JFST 2017; 73(3): 61-66.
10) Karsli NG, Aytac A, Effects of maleated polypropylene on the morphology, thermal and mechanical properties of short carbon fiber reinforced polypropylene composites. Mater Des 2011; 32(7): 4069-4073.
11) Lee H, Ohsawa I, Takahashi J. Effect of plasma surface treatment of recycled carbon fiber on carbon fiber-reinforced plastics (CFRP) interfacial properties. Appl Surf Sci 2015; 328: 241-246.
12) Li J. Interfacial studies on the O_3 modified carbon fiber-reinforced polyamide 6 composites. Appl

Surf Sci 2008; 255: 2822-2824.

13) Nishikawa M, Fukuzo A, Matsuda N, Hojo M. Muramatsu. Evaluation of elastic-plastic response of discontinuous carbon fiber-reinforced thermoplastics: Experiments and considerations based on load-transfer-based micromechanical simulation. Research of fiber length and fiber-matrix adhesion in carbon fiber reinforced polypropylene. Comp Sci Technol 2018; 155: 117-125.

14) Fujita R, Nagano H. Novel fiber orientation evaluation method for CFRP/CFRTP based on measurement of anisotropic in-plane thermal diffusivity distribution. Comp Sci Technol 2017; 140: 116-122.

15) Ishikawa T. Overview of carbon fiber reinforced composites (CFRP) applications to automotive structural parts, -focussed on thermoplastic CFRP-. J Jpn Soc Prec Engine 2015; 81(6): 489 -493.

16) Iyer SR, Drzal LT. Manufacture of powder-impregnated thermoplastic composites. J Therm Comp Mater 1990; 3(4): 325-355.

17) EL-Dessouky HM, Lawrence CA, Ultra-lightweight carbon fiber/thermoplastic composite material using spread tow technology. Composite part B 2013; 50: 91-97.

18) Lebrun G, Bureau MN, Denault J. Evaluation of bias-extension and picture-frame test methods for the measurement of intraply shear properties of PP/glass commingled fabrics. Compos Struct 2003; 61(4): 341-352.

19) Ben G, Ozeki H, Nakamura K, Hirayama N, Namaizawa M, Kobayashi M, Azuma H. Mechanical properties and molding conditions of CFRTP composed of carbon fabrics and *In-Situ* polymerizable thermoplastic resin. J Jpn Comp Mater 2013; 39(4): 127-134.

20) Ben G, Sakata K. Fast fabrication method and evaluation of performance of hybrid FRTPs for applying them to automotive structural members. Compos Struct 2015; 133 1160-1167.

21) Dai Z, Shi F, Zhang B, Li M, Zhang Z. Effect of sizing on carbon fiber surface properties and fibers/epoxy interfacial adhesion. Appl Surf Sci 2011; 257(15): 6980-6985.

22) Meyer LO, Schulte K, Grove-Nielsen E. CFRP-recycling following a pyrolysis route: process optimization and potentials. J Comps Mater 2009; 43(9): 1121-1132.

23) Irisawa T, Iwamura R, Kozawa Y, Kobayahi S, Tanabe Y. Recycling methods for

thermoplastic-matrix composites having high thermal stability in focusing on reuse of the carbon fibers. Tanso 2017; 280: 175-181.

24) Wada M, Kawai K, Suzuki T, Hira H, Kitaoka S. Effect of superheated steam treatment of carbon fiber on interfacial adhesion to epoxy resin. Composite Part A 2016; 85: 156-162.

25) Irisawa T, Takamura T, Momozono S, Kaneko J, Shioya M. Analysis on abrasive wear rate of VGCF/Polyamide 6 composite fibers. Tribology Online 2011; 6(4): 207-218.

26) Fornes TD, Paul DR. Crystallization behavior of nylon 6 nanocomposites. Polymer 2003; 44(14): 3945-3961.

27) Li J, Fang Z, Tong L, Gu A, Liu F. Polymorphism of nylon-6 in multiwalled carbon nanotubes/nylon-6 composites. J Polym Sci B 2006; 44(10): 1499-1512.

28) Ohsawa T, Nakayama TA, Miwa M, Hasegawa A. Temperature dependence of critical fiber length for glass fiber-reinforced thermosetting resins. J appl Polym Sci 1978; 22(11): 3203-3212.

29) Ogihara S, Koike Y, Maruyama K, Kobayashi S, Kogo Y. Effect of loading rate on fiber break behavior in a single carbon fiber reinforced plastic. J Soc Mater Sci Jpn 2004; 53(6): 667-672.

30) Yamamoto T, Uematsu K, Irisawa T, Tanabe Y. Controlling of the interfacial shear strength between thermoplastic resin and carbon fiber by adsorbing polymer particles on carbon fiber using electrophoresis. Composites Part A 2016; 88: 75-78.

31) Shioya M, Takaku A. Characterization of crystallites in carbon-fibers by wide-angle x-ray-diffraction. J Appl Crystallogr 1989; 22(3): 222–230.

32) Osbeck S, Bradley RH, Liu C, Idriss H, Ward S. Effect of an ultraviolet/ozone treatment on the surface texture and functional groups on polyacrylonitrile carbon fibres. Carbon 2011; 49(13): 4322-4330.

33) Edie DD. The effect of processing on the structure and properties of carbon fibers. Carbon 1998; 36(4): 345−362.

34) Shioya M, Shinotani K, Takaku A. Carbonization behavior of polyoxadiazole fibers and films. J. Mater. Sci. 1999; 34: 6015−6025.

35) Yang J, Liu J, Liu W, Wang J, Tang T. Recycling of carbon fiber reinforced epoxy resin composites

under various oxygen concentrations in nitrogen-oxygen atmosphere. J Analy Appl Pyroly 2015; 112: 253-261

36) Kim KW, Lee HM, An JH, Chung DC, An KH, Kim BJ. Recycling and characterization of carbon fibers from carbon fiber reinforced epoxy matrix composites by a novel super-heated-steam method. J Environ Manag 2017; 203(3): 872-879.

Table 1 The tensile modulus (E_f), strength (σ_f), density (d), crystallite parameters and O/C value of each Fre-CFs.

CFs code	Tensile test (N =50)		Sink-flow	WAXD			XPS
	E_f	σ_f	d	d_{002}	L_c	f	O/C
	(GPa)	(GPa)	(g/cm^3)	(nm)	(nm)	(-)	(-)
Fre-without-CFs	199 ± 9	4.2 ± 1.0	1.78	0.353	1.7	0.81	0.030
Fre-with-CFs	201 ± 8	4.8 ± 1.2	1.79	0.354	1.8	0.80	0.192
Fre-with-UV-CFs	205 ± 13	4.3 ± 1.0	1.79	0.352	1.7	0.82	0.113

The numbers after "±" are standard deviations.

Table 2 The melting temperature (T_m), crystallization temperature (T_c), crystallinity (X_c) and weight-average molecular weight (M_w) of PA6 into each CFRTPs.

CFRTPs code	DSC			GPC
	T_m	T_c	X_c	M_w
	(^{o}C)	(^{o}C)	(%)	(10^4)
Neat-PA6-RTM	213.4	175.7	26.6	7.7
Fre-without-CFs/CFRTP	213.8	183.7	32.3	7.8
Fre-with-CFs/CFRTP	214.6	180.1	27.9	8.6
Fre-with-UV-CFs/CFRP	214.6	178.5	27.7	10.5

Table 3 The tensile/bending modulus (E_c) and strength (σ_c) of each CFRTPs.

CFRTPs code	Volume Fraction of fiber (%)	Tensile test		Bending test	
		E_c (GPa) (N =8)	σ_c (MPa)	E_c (GPa) (N =8)	σ_c (MPa)
Fre-without-CFs/CFRTP	59 ± 4	59.9 ± 1.3	638 ± 28	49.0 ± 0.8	366 ± 23
Fre-with-CFs/CFRTP	61 ± 6	64.7 ± 8.7	705 ± 82	44.7 ± 1.0	463 ± 9
Fre-with-UV-CFs/CFRTP	57 ± 3	61.2 ± 1.5	749 ± 96	51.0 ± 3.1	509 ± 13

The numbers after "±" are standard deviations.

Table 4 The tensile modulus (E_f), strength (σ_f), density (d), crystallite parameters and O/C value of each Re-CFs.

CFs code	Tensile test (N=50)		Sink-flow	WAXD			XPS
	E_f (GPa)	σ_f (GPa)	d (g/cm^3)	d_{002} (nm)	L_c (nm)	f (-)	O/C (-)
Re-without-CFs	203 ± 10	4.1 ± 0.9	1.80	0.354	1.8	0.80	0.034
Re-with-CFs	203 ± 8	4.2 ± 1.1	1.81	0.355	1.7	0.79	0.058
Re-with-UV-CFs	203 ± 10	4.0 ± 1.0	1.80	0.353	1.7	0.81	0.068

The numbers after "±" are standard deviations.

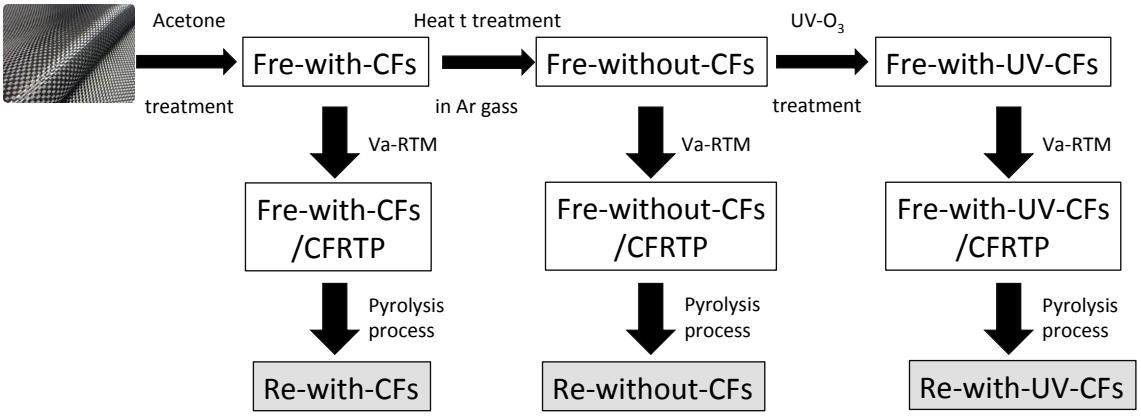

Fig. 1 Total flow chart of the preparation of Fre-CFs, CFRTPs and Re-CFs.

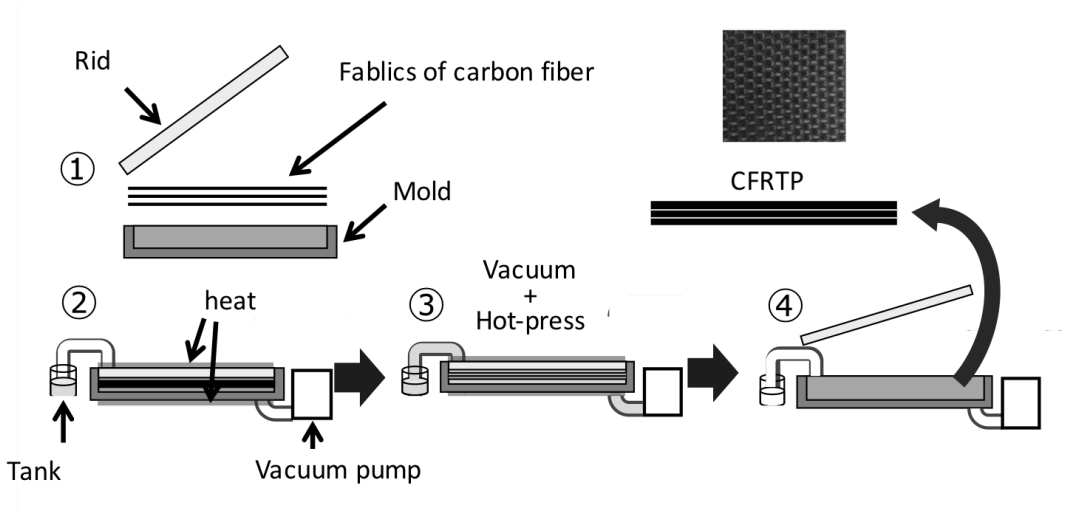

Fig. 2 Schematic illustration of Va-RTM methods.

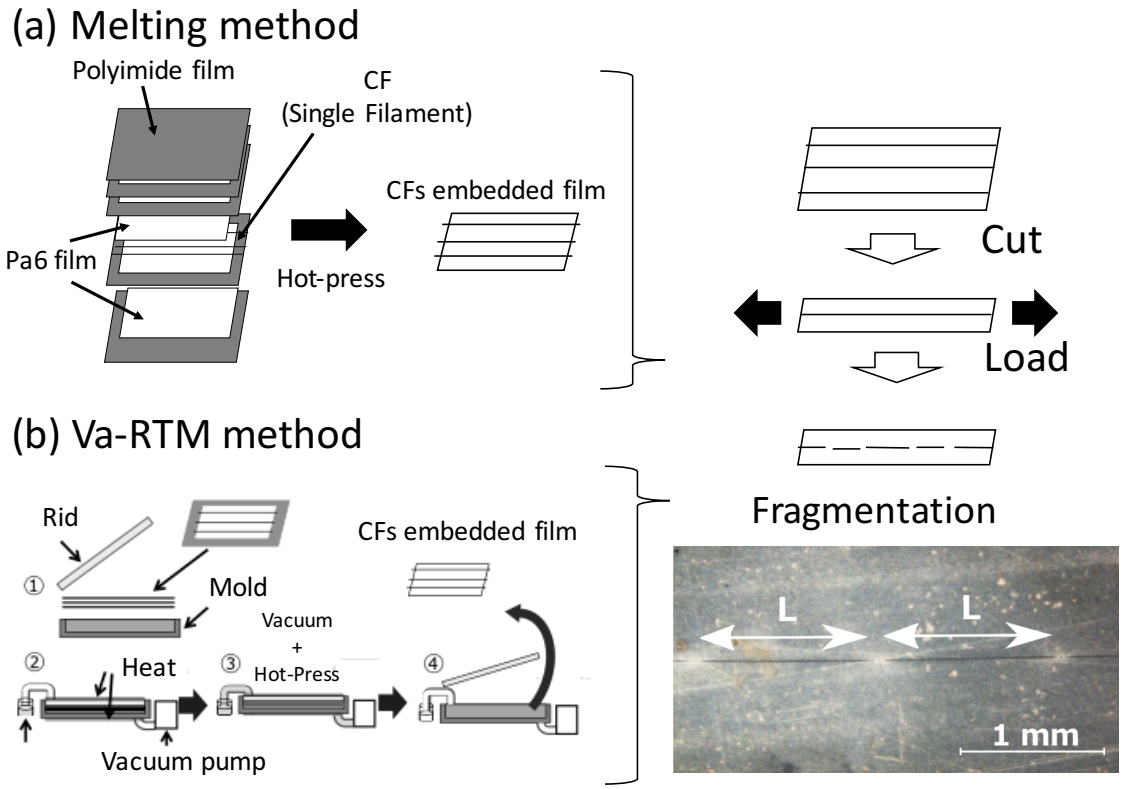

Fig. 3 Schematic illustration of fragmentation test procedure.

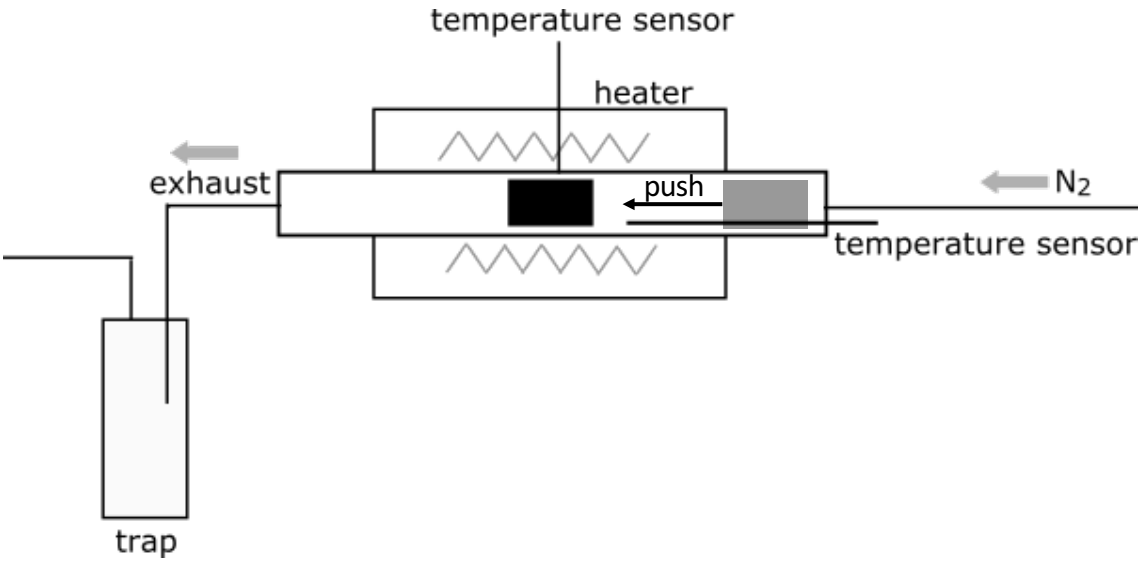

Fig. 4 Schematic illustration of tubular furnace for using pyrolytic process to recover the recycled CFs.

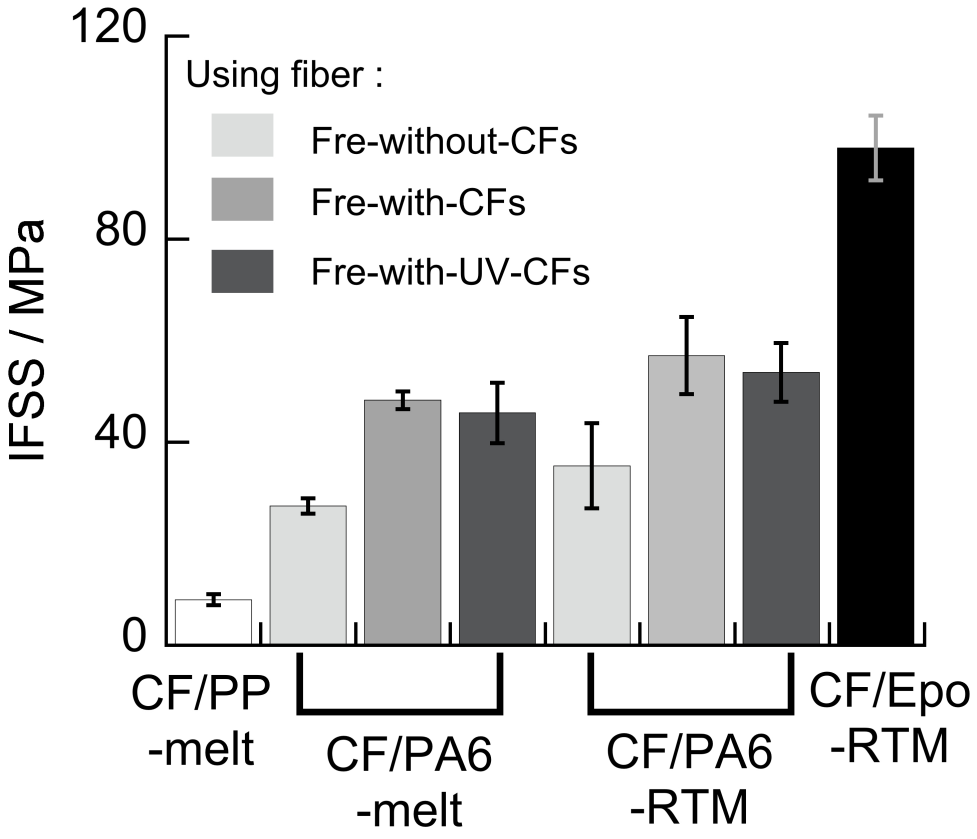

Fig. 5 The IFSS of CF/PP-melt, CF/PA6-melt, CF/PA6-RTM and CF/Epo-RTM. The error bars mean the standard deviations.

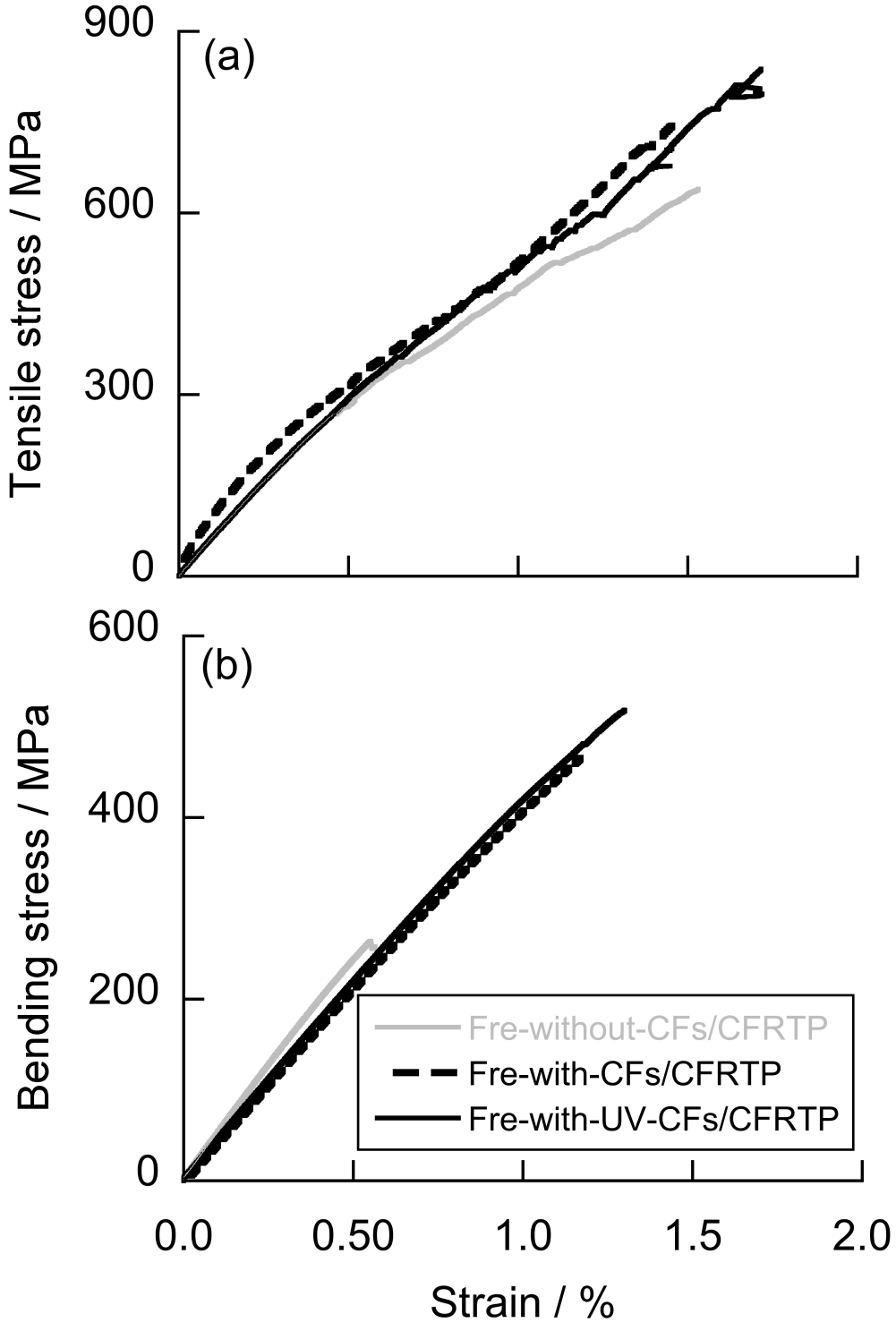

Fig. 6 The typical S-S curves of tensile/bending tests for each CFRTPs.

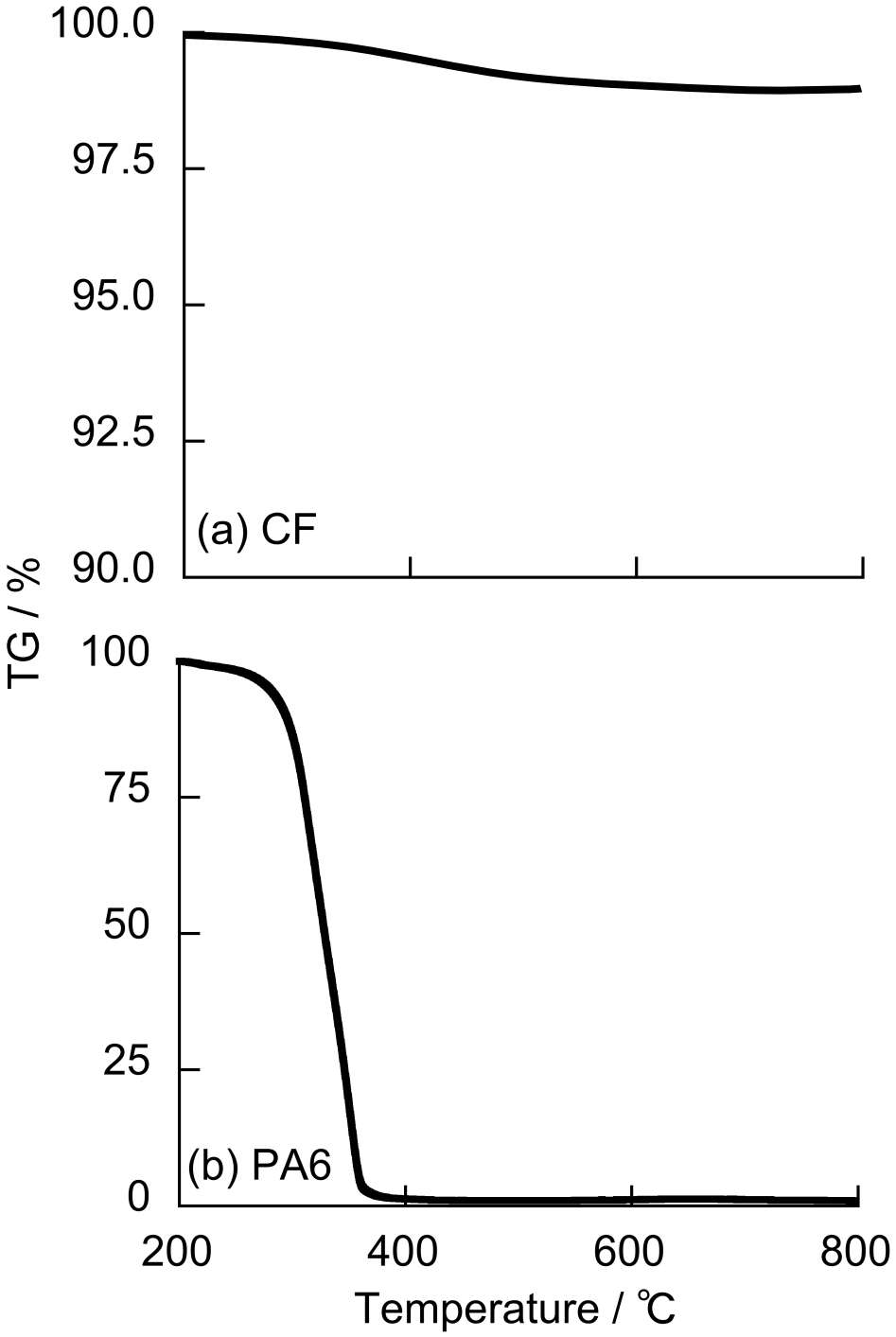

Fig. 7 TGA curves of (a) Fre-with-CFs and (b) Neat-PA6-RTM under N_2 gas.

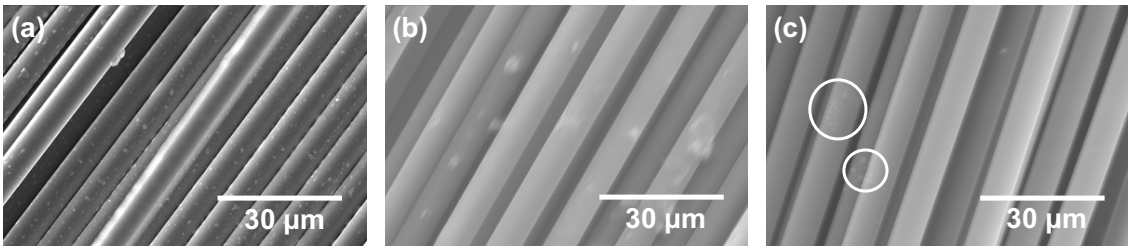

Fig. 8 SEM images of Re-with-CFs pyrolyzed from Fre-with-CFs/CFRTP at the temperature of (a) 500, (b) 550 and (c) 600 ºC for 30min under N_2 gas.

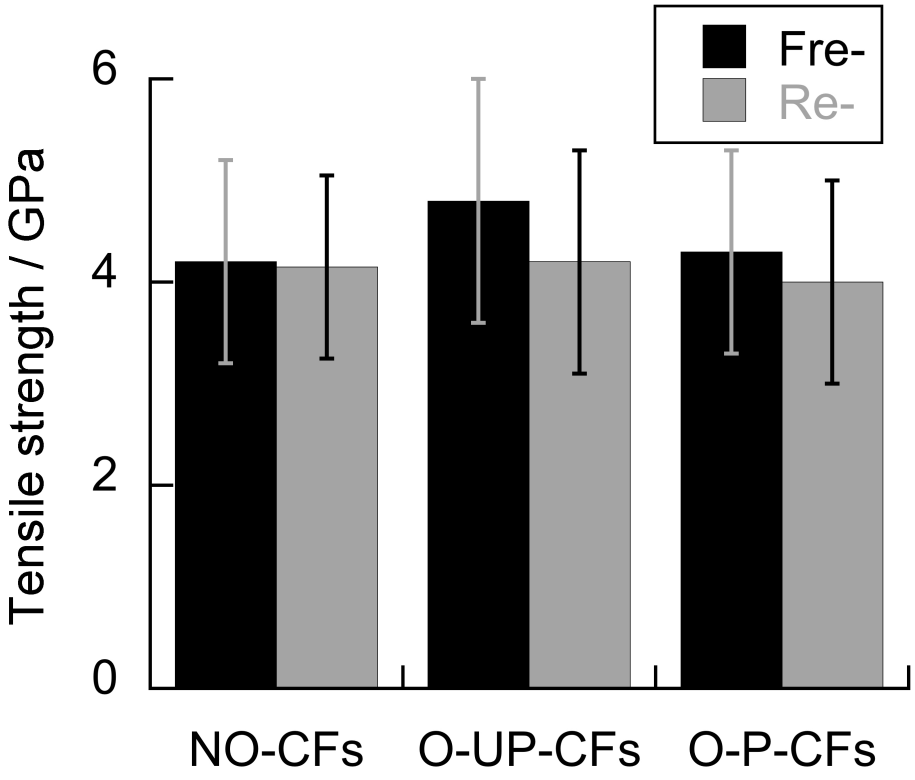

Fig. 9 The comparison of the tensile strength of Fre-CFs and Re-CFs. The error bars mean the standard deviations.

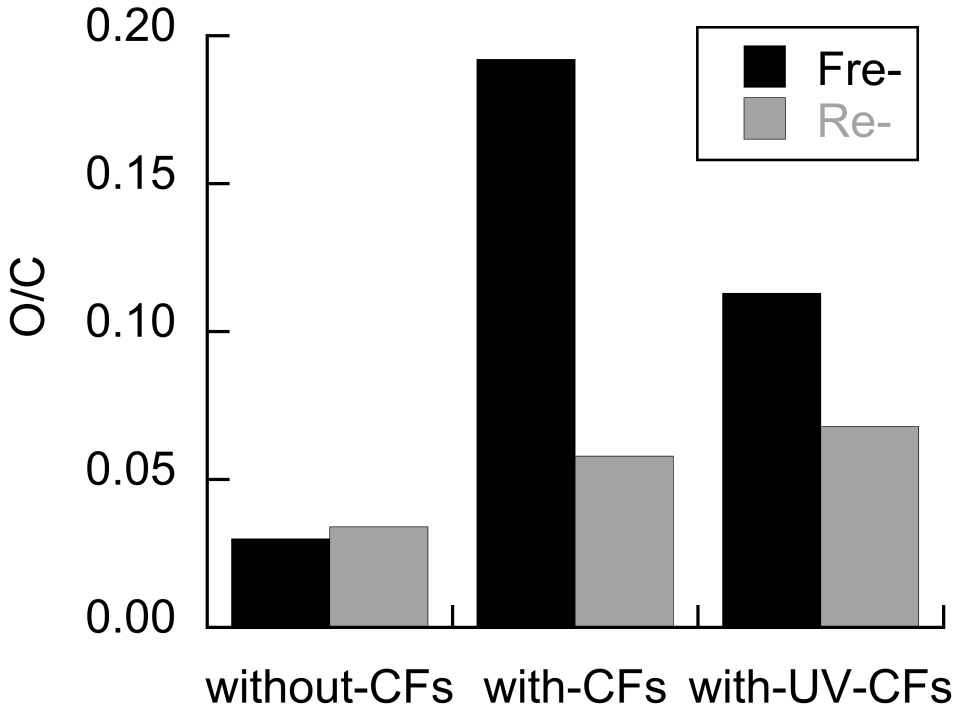

Fig. 10 The comparison of the O/C value of Fre-CFs and Re-CFs. The error bars mean the standard deviations.

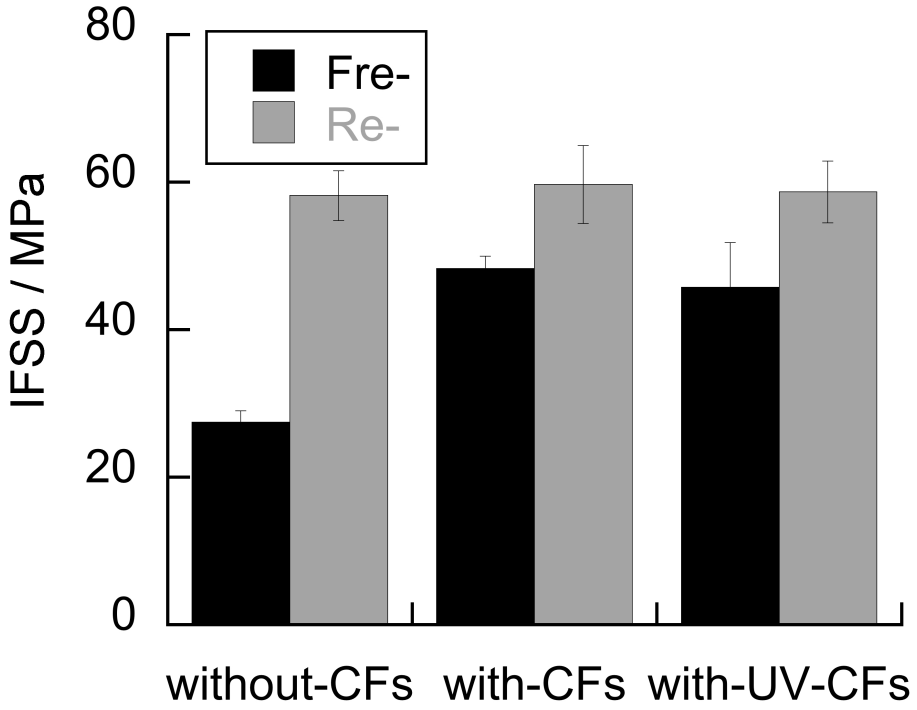

Fig. 11 The comparison of the IFSS of Fre-CFs and Re-CFs. The error bars mean the standard deviations.